I. INTRODUCTION

This brief communication focused on continuing the work of Rath et. al[1]. The paper does mainly concentrate on gradient driven flux-tub simulations close to the non-linear threshold and the occurrence of the E×B staircase structure and its formation over the simulation. At the end Section IV it was discussed that the circumstances for which the staircase can fully develop are beyond the scope of the paper. To gain more knowledge if the staircase structure can fully develop the following paper will focus on the effects of the box size on the E×B staircase structure and if the wavelength converges with the box size.

It is known that radially sheared zonal flows plays a significant role in nonlinear stabilization in tokamak plasmas.[2–4]. Through advection on the sheared zonal flows the turbulent structure in plasma gets deformed and tilted that causes an E×B nonlinearty.[3,5,6] The strength of the shearing process is the E×B shearing rate $\omega_{\mathrm{E\times B}}$ which is the radial derivative of the advecting zonal flow velocity.[5,7] The shearing rate $\omega_{\mathrm{E\times B}}$ is defined as

$$\omega_{\mathrm{E\times B}} = \frac{1}{2B}\frac{\partial^2\langle\Phi\rangle}{\partial\psi^2} \tag{1}$$

where $\langle\Phi\rangle$ is the zonal electrostatic potential and ψ the radial coordinate that labels the flux surfaces.[8,9] It was shown that the nonlinear threshold for turbulence is directly related to shear stabilization.[4] Often the shear stabilization is expressed in the empirical Waltz rule $\omega_{\mathrm{E\times B}} \sim \gamma$,[7,10] where γ is defined as the maximum linear growth rate in the unstable mode. In the discovered zonal flows, also known as E×B staircase[11], exhibit amplitudes in terms of the E×B shearing rate satisfying the stabilization criteria and for a fully developed staircase structure the E × B shearing rate $\omega_{\mathrm{E\times B}} = \gamma$.[1,8]

II. SIMULATION SETUP

The plasma parameters are nearly the same as in Ref 1 with the cyclone base case: safety factor $q = 1.4$, magnetic shear $\hat{s} = 0.78$, inverse aspect ratio $\varepsilon = 0.19$, density gradient $R/L_n = 2.2$ and electron to ion temperature ratio $T_e/T_i = 1$. The maximum of the velocity grid is three times the thermal velocity for both the parallel and the perpendicular velocities and adiabatic electrons with neglected collisions were investigated. For this paper the resolution "Standard resolution with 6th order (S6)" from Ref 1 was used and is given in Table I with changes in $N_{v_\parallel}$ from 64 grid points to 48 to reduces the runtime of simulations. Simulations showed that this correction in grid points does not affect the simulation itself.

The simulations are performed with the flux tube version of the non-linear gyro-kinetic code GKW.[12] Futher informations regarding the simulation can be found in Ref 1.

TABLE I: Resolution used in this paper (for more informations about the parameter read Ref 1)

	N_m	N_x	N_s	$N_{v_\parallel}$	N_μ	D	ν_d	$D_{v_\parallel}$	D_x	D_y	Order	$k_y\rho$	$k_x\rho$
S6	21	83	16	48	9	1	$\lvert v_\parallel\rvert$	0.2	0.1	0.1	6	1.4	2.1

III. RESULTS

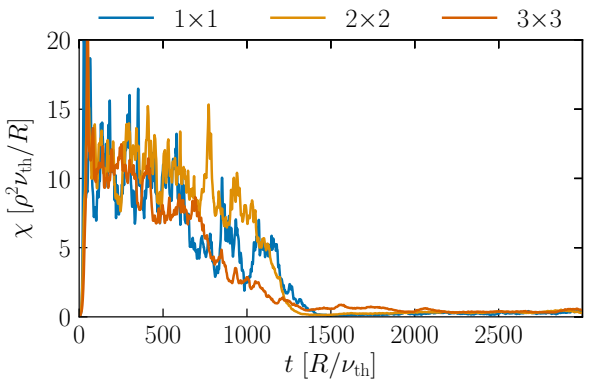

FIG. 1: Time traces of the heat conduction coefficient χ for $R/L_T = 6.0$ for radial and binormal increased boxsizes

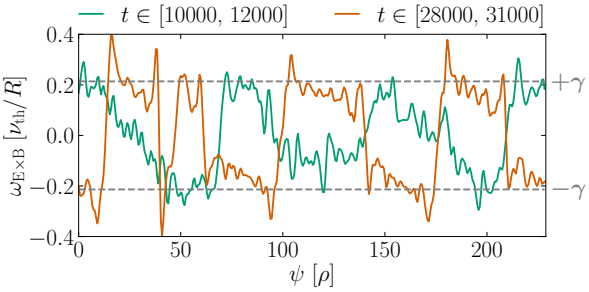

FIG. 2: Shearing rate $\omega_{\mathrm{E\times B}}$ for different time intervals in which heat conduction is almost zero but staircase has not fully developed for boxsize 3×1

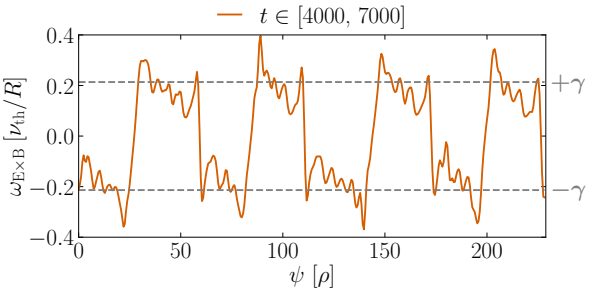

FIG. 3: Stablized shearing rate $\omega_{\mathrm{E\times B}}$ for boxsize 3×3

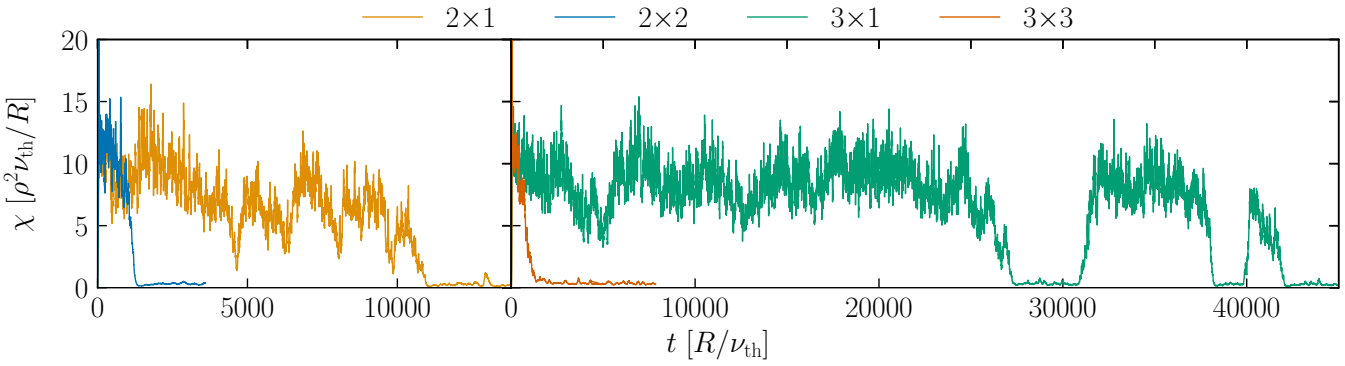

FIG. 4: Comparison of time traces of the heat conduction coefficient χ for $R/L_T = 6.0$ for boxsize 2×1 compared to 2×2 and 3×1 compared to 3×3

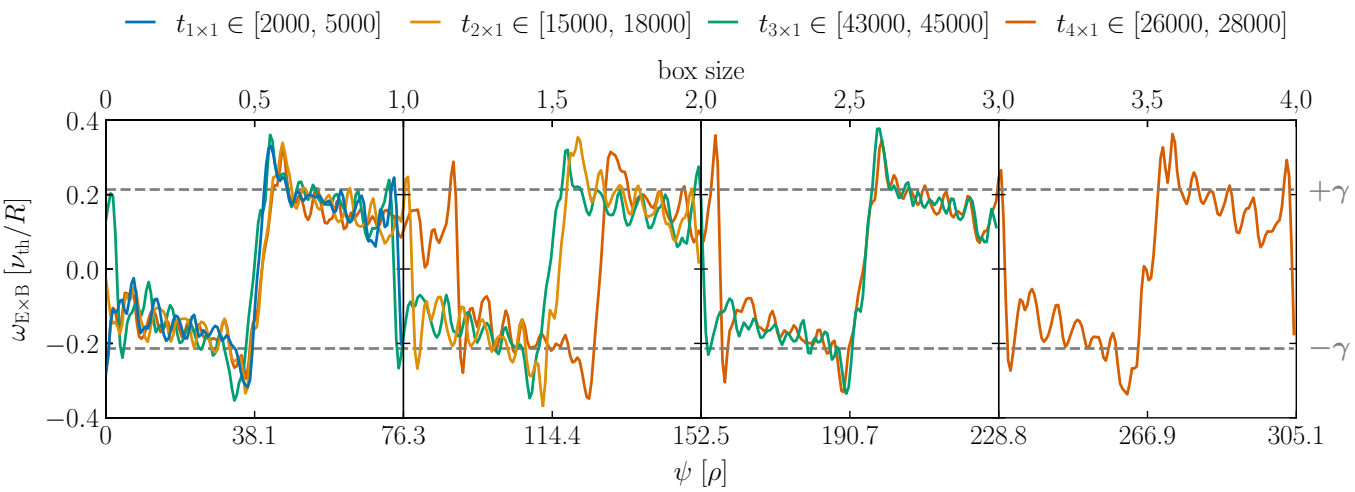

FIG. 5: Comparison of shearing rate $\omega_{\mathrm{E\times B}}$ for radial increased boxsizes. The staircase structure got shifted for better visibility.

IV. CONCLUSION

DATA AVAILABILITY

The data that support the findings of this study are available from the corresponding author upon reasonable request.

	Counter		Words	
	1 Col	2 Col	1 Col	2 Col
Words	———		674	
Figure	3	4	200	400
Table	0	0	13	26
Table Row	0	0	5	13
Eq Row	0	0	7	13
Pages	———		**3**	
Total	———		**2874**	
Remain	———		**626**	

[1] A. G. Peeters, F. Rath, R. Buchholz, Y. Camenen, J. Candy, F. J. Casson, S. R. Grosshauser, W. A. Hornsby, D. Strintzi, and A. Weikl, "Gradient-driven flux-tube simulations of ion temperature gradient turbulence close to the non-linear threshold," Phys. Plasmas **23**, 082517 (2016).
[2] W. A. Cooper, Plasma Physics and Controlled Fusion **30**, 1805 (1988).
[3] H. Biglari, P. H. Diamond, and P. W. Terry, Phys. Fluids B: Plasma Physics **2**, 1–4 (1990).
[4] A. M. Dimits, G. Bateman, M. A. Beer, B. I. Cohen, W. Dorland, G. W. Hammett, C. Kim, J. E. Kinsey, M. Kotschenreuther, A. H. Kritz, L. L. Lao, J. Mandrekas, W. M. Nevins, S. E. Parker, A. J. Redd, D. E. Shumaker, R. Sydora, and J. Weiland, "Comparisons and physics basis of tokamak transport models and turbulence simulations," Phys. of Plasmas **7**, 969–983 (2000).
[5] T. S. Hahm and K. H. Burrell, "Flow shear induced fluctuation suppression in finite aspect ratio shaped tokamak plasma," Phys. Plasmas **2**, 1648–1651 (1995).
[6] K. H. Burrell, Phys. Plasmas **4**, 1499–1518 (1997).
[7] R. E. Waltz, R. L. Dewar, and X. Garbet, Phys. Plasmas **5**, 1784–1792 (1998).
[8] F. Rath, A. G. Peeters, R. Buchholz, S. R. Grosshauser, P. Migliano, A. Weikl, and D. Strintzi, "Comparison of gradient and flux driven gyro-kinetic turbulent transport," Phys. Plasmas **23**, 052309 (2016).
[9] M. J. Pueschel, M. Kammerer, and F. Jenko, Physics of Plasmas **15**, 102310 (2008).
[10] R. E. Waltz, G. D. Kerbel, and J. Milovich, Phys. Plasmas **1**, 2229 (1994).
[11] G. Dif-Pradalier, P. H. Diamond, V. Grandgirard, Y. Sarazin, J. Abiteboul, X. Garbet, P. Ghendrih, A. Strugarek, S. Ku, and C. S. Chang, Phys. Rev. E **82**, 025401 (2010).
[12] A. G. Peeters, Y. Camenen, F. J. Casson, W. A. Hornsby, A. P. Snodin, D. Strintzi, and G. Szepesi, Comput. Phys. Commun. **180**, 2650 (2009).

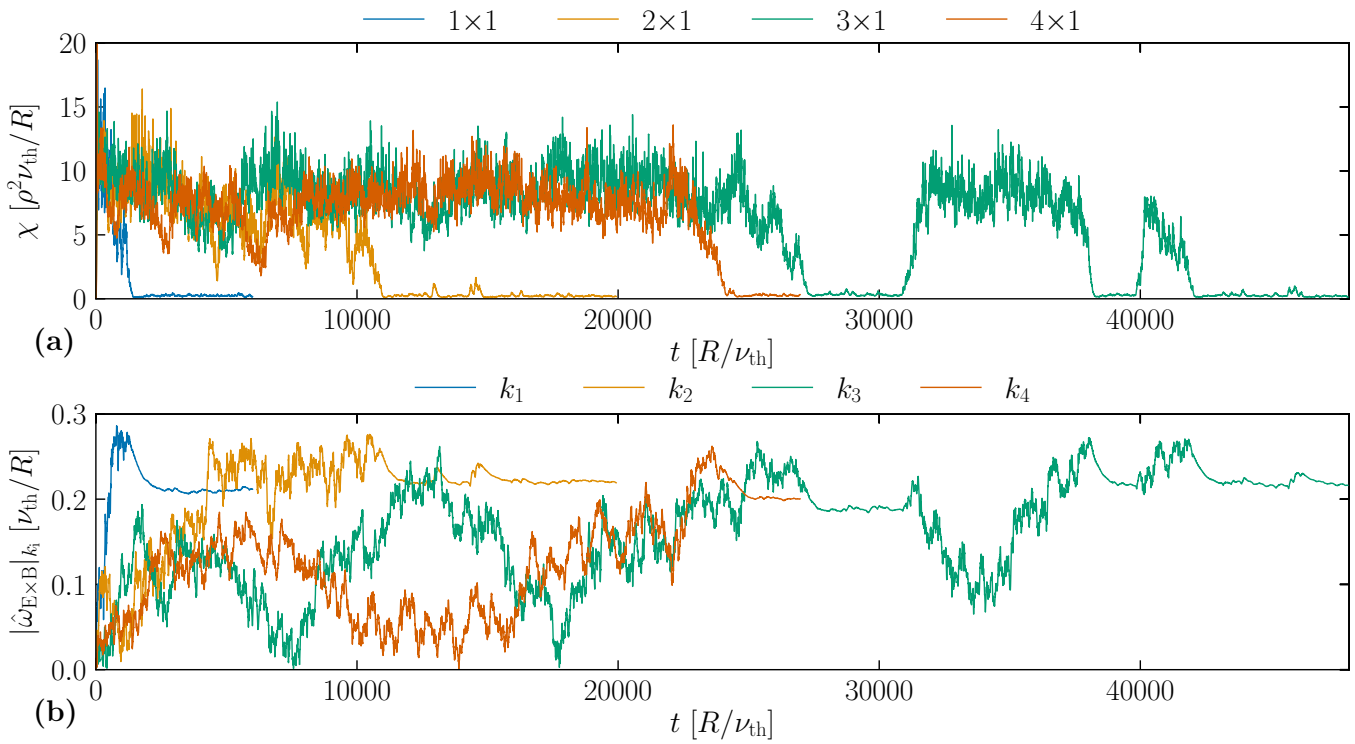

FIG. 6: **(a)** Time traces of the heat conduction coefficient χ for $R/L_T = 6.0$ for radial increased boxsizes
(b) Time traces of $|\hat{\omega}_{\mathrm{E\times B}}|_{k_i}$ for radial increased boxsizes